First Observation of the Direct Production of the χ_{c1} in e^+e^- Annihilation

M. Ablikim,[1] M. N. Achasov,[10,b] P. Adlarson,[69] S. Ahmed,[15] M. Albrecht,[4] R. Aliberti,[29] A. Amoroso,[68a,68c] M. R. An,[33] Q. An,[65,51] X. H. Bai,[59] Y. Bai,[50] O. Bakina,[30] R. Baldini Ferroli,[24a] I. Balossino,[25a] Y. Ban,[40,i] V. Batozskaya,[1,38] D. Becker,[29] K. Begzsuren,[27] N. Berger,[29] M. Bertani,[24a] D. Bettoni,[25a] F. Bianchi,[68a,68c] J. Bloms,[62] A. Bortone,[68a,68c] I. Boyko,[30] R. A. Briere,[5] A. Brueggemann,[62] H. Cai,[70] X. Cai,[1,51] A. Calcaterra,[24a] G. F. Cao,[1,56] N. Cao,[1,56] S. A. Cetin,[55a] J. F. Chang,[1,51] W. L. Chang,[1,56] G. Chelkov,[30,a] C. Chen,[37] G. Chen,[1] H. S. Chen,[1,56] M. L. Chen,[1,51] S. J. Chen,[36] T. Chen,[1] X. R. Chen,[26] X. T. Chen,[1] Y. B. Chen,[1,51] Z. J. Chen,[21,j] W. S. Cheng,[68c] G. Cibinetto,[25a] F. Cossio,[68c] J. J. Cui,[43] H. L. Dai,[1,51] J. P. Dai,[72] A. Dbeyssi,[15] R. E. de Boer,[4] D. Dedovich,[30] Z. Y. Deng,[1] A. Denig,[29] I. Denysenko,[30] M. Destefanis,[68a,68c] F. De Mori,[68a,68c] Y. Ding,[34] J. Dong,[1,51] L. Y. Dong,[1,56] M. Y. Dong,[1,51,56] X. Dong,[70] S. X. Du,[74] P. Egorov,[30,a] Y. L. Fan,[70] J. Fang,[1,51] S. S. Fang,[1,56] Y. Fang,[1] R. Farinelli,[25a] L. Fava,[68b,68c] F. Feldbauer,[4] G. Felici,[24a] C. Q. Feng,[65,51] J. H. Feng,[52] M. Fritsch,[4] C. D. Fu,[1] H. Gao,[56,h] Y. N. Gao,[40,i] Yang Gao,[65,51] I. Garzia,[25a,25b] P. T. Ge,[70] C. Geng,[52] E. M. Gersabeck,[60] A. Gilman,[63] K. Goetzen,[11] L. Gong,[34] W. X. Gong,[1,51] W. Gradl,[29] M. Greco,[68a,68c] M. H. Gu,[1,51] Y. T. Gu,[13] C. Y. Guan,[1,56] A. Q. Guo,[26] L. B. Guo,[35] R. P. Guo,[42] Y. P. Guo,[9,g] A. Guskov,[30,a] T. T. Han,[43] W. Y. Han,[33] X. Q. Hao,[16] F. A. Harris,[58] K. K. He,[48] K. L. He,[1,56] F. H. Heinsius,[4] C. H. Heinz,[29] Y. K. Heng,[1,51,56] C. Herold,[53] M. Himmelreich,[11,e] T. Holtmann,[4] G. Y. Hou,[1,56] Y. R. Hou,[56] Z. L. Hou,[1] H. M. Hu,[1,56] J. F. Hu,[49,k] T. Hu,[1,51,56] Y. Hu,[1] G. S. Huang,[65,51] K. X. Huang,[52] L. Q. Huang,[66] X. T. Huang,[43] Y. P. Huang,[1] Z. Huang,[40,i] T. Hussain,[67] N. Hüsken,[23,29] W. Imoehl,[23] M. Irshad,[65,51] J. Jackson,[23] S. Jaeger,[4] S. Janchiv,[27] Q. Ji,[1] Q. P. Ji,[16] X. B. Ji,[1,56] X. L. Ji,[1,51] Y. Y. Ji,[43] H. B. Jiang,[43] S. S. Jiang,[33] X. S. Jiang,[1,51,56] Y. Jiang,[56] J. B. Jiao,[43] Z. Jiao,[19] S. Jin,[36] Y. Jin,[59] M. Q. Jing,[1,56] T. Johansson,[69] N. Kalantar-Nayestanaki,[57] X. S. Kang,[34] R. Kappert,[57] M. Kavatsyuk,[57] B. C. Ke,[74] I. K. Keshk,[4] A. Khoukaz,[62] P. Kiese,[29] R. Kiuchi,[1] R. Kliemt,[11] L. Koch,[31] O. B. Kolcu,[55a] B. Kopf,[4] M. Kuemmel,[4] M. Kuessner,[4] A. Kupsc,[38,69] W. Kühn,[31] J. J. Lane,[60] J. S. Lange,[31] P. Larin,[15] A. Lavania,[22] L. Lavezzi,[68a,68c] Z. H. Lei,[65,51] H. Leithoff,[29] M. Lellmann,[29] T. Lenz,[29] C. Li,[37] C. Li,[41] C. H. Li,[33] Cheng Li,[65,51] D. M. Li,[74] F. Li,[1,51] G. Li,[1] H. Li,[65,51] H. Li,[45] H. B. Li,[1,56] H. J. Li,[16] H. N. Li,[49,k] J. Q. Li,[4] J. S. Li,[52] J. W. Li,[43] Ke Li,[1] L. J. Li,[1] L. K. Li,[1] Lei Li,[3] M. H. Li,[37] P. R. Li,[32,l,m] S. X. Li,[9] S. Y. Li,[54] T. Li,[43] W. D. Li,[1,56] W. G. Li,[1] X. H. Li,[65,51] X. L. Li,[43] Xiaoyu Li,[1,56] Z. Y. Li,[52] H. Liang,[28] H. Liang,[1,56] H. Liang,[65,51] Y. F. Liang,[47] Y. T. Liang,[26] G. R. Liao,[12] L. Z. Liao,[43] J. Libby,[22] A. Limphirat,[53] C. X. Lin,[52] D. X. Lin,[26] T. Lin,[1] B. J. Liu,[1] C. X. Liu,[1] D. Liu,[15,65] F. H. Liu,[46] Fang Liu,[1] Feng Liu,[6] G. M. Liu,[49,k] H. B. Liu,[13] H. M. Liu,[1,56] Huanhuan Liu,[1] Huihui Liu,[17] J. B. Liu,[65,51] J. L. Liu,[66] J. Y. Liu,[1,56] K. Liu,[1] K. Y. Liu,[34] Ke Liu,[18] L. Liu,[65,51] M. H. Liu,[9,g] P. L. Liu,[1] Q. Liu,[56] S. B. Liu,[65,51] T. Liu,[9,g] W. K. Liu,[37] W. M. Liu,[65,51] X. Liu,[32,l,m] Y. Liu,[32,l,m] Y. B. Liu,[37] Z. A. Liu,[1,51,56] Z. Q. Liu,[43] X. C. Lou,[1,51,56] F. X. Lu,[52] H. J. Lu,[19] J. G. Lu,[1,51] X. L. Lu,[1] Y. Lu,[1] Y. P. Lu,[1,51] Z. H. Lu,[1] C. L. Luo,[35] M. X. Luo,[73] T. Luo,[9,g] X. L. Luo,[1,51] X. R. Lyu,[56] Y. F. Lyu,[37] F. C. Ma,[34] H. L. Ma,[1] L. L. Ma,[43] M. M. Ma,[1,56] Q. M. Ma,[1] R. Q. Ma,[1,56] R. T. Ma,[56] X. Y. Ma,[1,51] Y. Ma,[40,i] F. E. Maas,[15] M. Maggiora,[68a,68c] S. Maldaner,[4] S. Malde,[63] Q. A. Malik,[67] A. Mangoni,[24b] Y. J. Mao,[40,i] Z. P. Mao,[1] S. Marcello,[68a,68c] Z. X. Meng,[59] J. G. Messchendorp,[57,d] G. Mezzadri,[25a] H. Miao,[1] T. J. Min,[36] R. E. Mitchell,[23] X. H. Mo,[1,51,56] N. Yu. Muchnoi,[10,b] H. Muramatsu,[61] S. Nakhoul,[11,e] Y. Nefedov,[30] F. Nerling,[11,e] I. B. Nikolaev,[10,b] Z. Ning,[1,51] S. Nisar,[8,n] Y. Niu,[43] S. L. Olsen,[56] Q. Ouyang,[1,51,56] S. Pacetti,[24b,24c] X. Pan,[9,g] Y. Pan,[60] A. Pathak,[1] A. Pathak,[28] P. Patteri,[24a] M. Pelizaeus,[4] H. P. Peng,[65,51] K. Peters,[11,e] J. Pettersson,[69] J. L. Ping,[35] R. G. Ping,[1,56] S. Plura,[29] S. Pogodin,[30] R. Poling,[61] V. Prasad,[65,51] H. Qi,[65,51] H. R. Qi,[54] M. Qi,[36] T. Y. Qi,[9,g] S. Qian,[1,51] W. B. Qian,[56] Z. Qian,[52] C. F. Qiao,[56] J. J. Qin,[66] L. Q. Qin,[12] X. P. Qin,[9,g] X. S. Qin,[43] Z. H. Qin,[1,51] J. F. Qiu,[1] S. Q. Qu,[54] K. H. Rashid,[67] K. Ravindran,[22] C. F. Redmer,[29] K. J. Ren,[33] A. Rivetti,[68c] V. Rodin,[57] M. Rolo,[68c] G. Rong,[1,56] Ch. Rosner,[15] M. Rump,[62] H. S. Sang,[65] A. Sarantsev,[30,c] Y. Schelhaas,[29] C. Schnier,[4] K. Schoenning,[69] M. Scodeggio,[25a,25b] K. Y. Shan,[9,g] W. Shan,[20] X. Y. Shan,[65,51] J. F. Shangguan,[48] L. G. Shao,[1,56] M. Shao,[65,51] C. P. Shen,[9,g] H. F. Shen,[1,56] X. Y. Shen,[1,56] B.-A. Shi,[56] H. C. Shi,[65,51] R. S. Shi,[1,56] X. Shi,[1,51] X. D. Shi,[65,51] J. J. Song,[16] W. M. Song,[28,1] Y. X. Song,[40,i] S. Sosio,[68a,68c] S. Spataro,[68a,68c] F. Stieler,[29] K. X. Su,[70] P. P. Su,[48] Y.-J. Su,[56] G. X. Sun,[1] H. Sun,[56] H. K. Sun,[1] J. F. Sun,[16] L. Sun,[70] S. S. Sun,[1,56] T. Sun,[1,56] W. Y. Sun,[28] X. Sun,[21,j] Y. J. Sun,[65,51] Y. Z. Sun,[1] Z. T. Sun,[43] Y. H. Tan,[70] Y. X. Tan,[65,51] C. J. Tang,[47] G. Y. Tang,[1] J. Tang,[52] Q. T. Tao,[21,j] J. X. Teng,[65,51] V. Thoren,[69] W. H. Tian,[45] Y. T. Tian,[26] I. Uman,[55b] B. Wang,[1] D. Y. Wang,[40,i] H. J. Wang,[32,l,m] H. P. Wang,[1,56] K. Wang,[1,51] L. L. Wang,[1] M. Wang,[43] M. Z. Wang,[40,i] Meng Wang,[1,56] S. Wang,[9,g] T. J. Wang,[37] W. Wang,[52] W. H. Wang,[70] W. P. Wang,[65,51] X. Wang,[40,i] X. F. Wang,[32,l,m] X. L. Wang,[9,g] Y. D. Wang,[39] Y. F. Wang,[1,51,56] Y. Q. Wang,[1] Y. Y. Wang,[32,l,m] Ying Wang,[52] Z. Wang,[1,51] Z. Y. Wang,[1] Ziyi Wang,[56] D. H. Wei,[12] F. Weidner,[62] S. P. Wen,[1] D. J. White,[60] U. Wiedner,[4] G. Wilkinson,[63] M. Wolke,[69] L. Wollenberg,[4] J. F. Wu,[1,56] L. H. Wu,[1] L. J. Wu,[1,56] X. Wu,[9,g] X. H. Wu,[28]

Y. Wu,[65] Z. Wu,[1,51] L. Xia,[65,51] T. Xiang,[40,i] H. Xiao,[9,g] S. Y. Xiao,[1] Y. L. Xiao,[9,g] Z. J. Xiao,[35] X. H. Xie,[40,i] Y. Xie,[43] Y. G. Xie,[1,51] Y. H. Xie,[6] Z. P. Xie,[65,51] T. Y. Xing,[1,56] C. F. Xu,[1] C. J. Xu,[52] G. F. Xu,[1] Q. J. Xu,[14] S. Y. Xu,[64] X. P. Xu,[48] Y. C. Xu,[56] F. Yan,[9,g] L. Yan,[9,g] W. B. Yan,[65,51] W. C. Yan,[74] H. J. Yang,[44,f] H. X. Yang,[1] L. Yang,[45] S. L. Yang,[56] Y. X. Yang,[1,56] Yifan Yang,[1,56] Zhi Yang,[26] M. Ye,[1,51] M. H. Ye,[7] J. H. Yin,[1] Z. Y. You,[52] B. X. Yu,[1,51,56] C. X. Yu,[37] G. Yu,[1,56] J. S. Yu,[21,j] T. Yu,[66] C. Z. Yuan,[1,56] L. Yuan,[2] S. C. Yuan,[1] X. Q. Yuan,[1] Y. Yuan,[1,56] Z. Y. Yuan,[52] C. X. Yue,[33] A. A. Zafar,[67] F. R. Zeng,[43] X. Zeng,[6] Y. Zeng,[21,j] Y. H. Zhan,[52] A. Q. Zhang,[1] B. L. Zhang,[1] B. X. Zhang,[1] G. Y. Zhang,[16] H. Zhang,[65] H. H. Zhang,[52] H. H. Zhang,[28] H. Y. Zhang,[1,51] J. L. Zhang,[71] J. Q. Zhang,[35] J. W. Zhang,[1,51,56] J. Y. Zhang,[1] J. Z. Zhang,[1,56] Jianyu Zhang,[1,56] Jiawei Zhang,[1,56] L. M. Zhang,[54] L. Q. Zhang,[52] Lei Zhang,[36] P. Zhang,[1] Shulei Zhang,[21,j] X. D. Zhang,[39] X. M. Zhang,[1] X. Y. Zhang,[48] X. Y. Zhang,[43] Y. Zhang,[63] Y. T. Zhang,[74] Y. H. Zhang,[1,51] Yan Zhang,[65,51] Yao Zhang,[1] Z. H. Zhang,[1] Z. Y. Zhang,[70] Z. Y. Zhang,[37] G. Zhao,[1] J. Zhao,[33] J. Y. Zhao,[1,56] J. Z. Zhao,[1,51] Lei Zhao,[65,51] Ling Zhao,[1] M. G. Zhao,[37] Q. Zhao,[1] S. J. Zhao,[74] Y. B. Zhao,[1,51] Y. X. Zhao,[26] Z. G. Zhao,[65,51] A. Zhemchugov,[30,a] B. Zheng,[66] J. P. Zheng,[1,51] Y. H. Zheng,[56] B. Zhong,[35] C. Zhong,[66] X. Zhong,[52] H. Zhou,[43] L. P. Zhou,[1,56] X. Zhou,[70] X. K. Zhou,[56] X. R. Zhou,[65,51] X. Y. Zhou,[33] J. Zhu,[37] K. Zhu,[1] K. J. Zhu,[1,51,56] L. X. Zhu,[56] S. H. Zhu,[64] T. J. Zhu,[71] W. J. Zhu,[9,g] W. J. Zhu,[37] Y. C. Zhu,[65,51] Z. A. Zhu,[1,56] B. S. Zou,[1] and J. H. Zou[1]

(BESIII Collaboration)

[1]*Institute of High Energy Physics, Beijing 100049, People's Republic of China*
[2]*Beihang University, Beijing 100191, People's Republic of China*
[3]*Beijing Institute of Petrochemical Technology, Beijing 102617, People's Republic of China*
[4]*Bochum Ruhr-University, D-44780 Bochum, Germany*
[5]*Carnegie Mellon University, Pittsburgh, Pennsylvania 15213, USA*
[6]*Central China Normal University, Wuhan 430079, People's Republic of China*
[7]*China Center of Advanced Science and Technology, Beijing 100190, People's Republic of China*
[8]*COMSATS University Islamabad, Lahore Campus, Defence Road, Off Raiwind Road, 54000 Lahore, Pakistan*
[9]*Fudan University, Shanghai 200433, People's Republic of China*
[10]*G.I. Budker Institute of Nuclear Physics SB RAS (BINP), Novosibirsk 630090, Russia*
[11]*GSI Helmholtzcentre for Heavy Ion Research GmbH, D-64291 Darmstadt, Germany*
[12]*Guangxi Normal University, Guilin 541004, People's Republic of China*
[13]*Guangxi University, Nanning 530004, People's Republic of China*
[14]*Hangzhou Normal University, Hangzhou 310036, People's Republic of China*
[15]*Helmholtz Institute Mainz, Staudinger Weg 18, D-55099 Mainz, Germany*
[16]*Henan Normal University, Xinxiang 453007, People's Republic of China*
[17]*Henan University of Science and Technology, Luoyang 471003, People's Republic of China*
[18]*Henan University of Technology, Zhengzhou 450001, People's Republic of China*
[19]*Huangshan College, Huangshan 245000, People's Republic of China*
[20]*Hunan Normal University, Changsha 410081, People's Republic of China*
[21]*Hunan University, Changsha 410082, People's Republic of China*
[22]*Indian Institute of Technology Madras, Chennai 600036, India*
[23]*Indiana University, Bloomington, Indiana 47405, USA*
[24a]*INFN Laboratori Nazionali di Frascati, INFN Laboratori Nazionali di Frascati, I-00044, Frascati, Italy*
[24b]*INFN Sezione di Perugia, I-06100, Perugia, Italy*
[24c]*University of Perugia, I-06100, Perugia, Italy*
[25a]*INFN Sezione di Ferrara, INFN Sezione di Ferrara, I-44122, Ferrara, Italy*
[25b]*University of Ferrara, I-44122, Ferrara, Italy*
[26]*Institute of Modern Physics, Lanzhou 730000, People's Republic of China*
[27]*Institute of Physics and Technology, Peace Avenue 54B, Ulaanbaatar 13330, Mongolia*
[28]*Jilin University, Changchun 130012, People's Republic of China*
[29]*Johannes Gutenberg University of Mainz, Johann-Joachim-Becher-Weg 45, D-55099 Mainz, Germany*
[30]*Joint Institute for Nuclear Research, 141980 Dubna, Moscow region, Russia*
[31]*Justus-Liebig-Universitaet Giessen, II. Physikalisches Institut, Heinrich-Buff-Ring 16, D-35392 Giessen, Germany*
[32]*Lanzhou University, Lanzhou 730000, People's Republic of China*
[33]*Liaoning Normal University, Dalian 116029, People's Republic of China*
[34]*Liaoning University, Shenyang 110036, People's Republic of China*
[35]*Nanjing Normal University, Nanjing 210023, People's Republic of China*
[36]*Nanjing University, Nanjing 210093, People's Republic of China*
[37]*Nankai University, Tianjin 300071, People's Republic of China*

[38]National Centre for Nuclear Research, Warsaw 02-093, Poland
[39]North China Electric Power University, Beijing 102206, People's Republic of China
[40]Peking University, Beijing 100871, People's Republic of China
[41]Qufu Normal University, Qufu 273165, People's Republic of China
[42]Shandong Normal University, Jinan 250014, People's Republic of China
[43]Shandong University, Jinan 250100, People's Republic of China
[44]Shanghai Jiao Tong University, Shanghai 200240, People's Republic of China
[45]Shanxi Normal University, Linfen 041004, People's Republic of China
[46]Shanxi University, Taiyuan 030006, People's Republic of China
[47]Sichuan University, Chengdu 610064, People's Republic of China
[48]Soochow University, Suzhou 215006, People's Republic of China
[49]South China Normal University, Guangzhou 510006, People's Republic of China
[50]Southeast University, Nanjing 211100, People's Republic of China
[51]State Key Laboratory of Particle Detection and Electronics, Beijing 100049, Hefei 230026, People's Republic of China
[52]Sun Yat-Sen University, Guangzhou 510275, People's Republic of China
[53]Suranaree University of Technology, University Avenue 111, Nakhon Ratchasima 30000, Thailand
[54]Tsinghua University, Beijing 100084, People's Republic of China
[55a]Turkish Accelerator Center Particle Factory Group, Istinye University, 34010, Istanbul, Turkey
[55b]Near East University, Nicosia, North Cyprus, Mersin 10, Turkey
[56]University of Chinese Academy of Sciences, Beijing 100049, People's Republic of China
[57]University of Groningen, NL-9747 AA Groningen, Netherlands
[58]University of Hawaii, Honolulu, Hawaii 96822, USA
[59]University of Jinan, Jinan 250022, People's Republic of China
[60]University of Manchester, Oxford Road, Manchester, M13 9PL, United Kingdom
[61]University of Minnesota, Minneapolis, Minnesota 55455, USA
[62]University of Muenster, Wilhelm-Klemm-Straße 9, 48149 Muenster, Germany
[63]University of Oxford, Keble Road, Oxford, United Kingdom OX13RH
[64]University of Science and Technology Liaoning, Anshan 114051, People's Republic of China
[65]University of Science and Technology of China, Hefei 230026, People's Republic of China
[66]University of South China, Hengyang 421001, People's Republic of China
[67]University of the Punjab, Lahore-54590, Pakistan
[68a]University of Turin and INFN, University of Turin, I-10125, Turin, Italy
[68b]University of Eastern Piedmont, I-15121, Alessandria, Italy
[68c]INFN, I-10125, Turin, Italy
[69]Uppsala University, Box 516, SE-75120 Uppsala, Sweden
[70]Wuhan University, Wuhan 430072, People's Republic of China
[71]Xinyang Normal University, Xinyang 464000, People's Republic of China
[72]Yunnan University, Kunming 650500, People's Republic of China
[73]Zhejiang University, Hangzhou 310027, People's Republic of China
[74]Zhengzhou University, Zhengzhou 450001, People's Republic of China

(Received 23 March 2022; revised 22 June 2022; accepted 26 July 2022; published 12 September 2022)

We study the direct production of the $J^{PC} = 1^{++}$ charmonium state $\chi_{c1}(1P)$ in electron-positron annihilation by carrying out an energy scan around the mass of the $\chi_{c1}(1P)$. The data were collected with the BESIII detector at the BEPCII collider. An interference pattern between the signal process $e^+e^- \to \chi_{c1}(1P) \to \gamma J/\psi \to \gamma\mu^+\mu^-$ and the background processes $e^+e^- \to \gamma_{\rm ISR} J/\psi \to \gamma_{\rm ISR}\mu^+\mu^-$ and $e^+e^- \to \gamma_{\rm ISR}\mu^+\mu^-$ is observed by combining all the data samples. The $\chi_{c1}(1P)$ signal is observed with a significance of 5.1σ. This is the first observation of a C-even state directly produced in e^+e^- annihilation. The electronic width of the $\chi_{c1}(1P)$ resonance is determined to be $\Gamma_{ee} = (0.12^{+0.13}_{-0.08})$ eV, which is of the same order of magnitude as theoretical calculations.

DOI: 10.1103/PhysRevLett.129.122001

In the process $e^+e^- \to R$, where R represents a hadronic resonance, the dominant production mechanism, when allowed, is through one virtual photon. This results in the copious production of vector mesons with $J^{PC} = 1^{--}$, where the quantum numbers J, P, and C denote the spin,

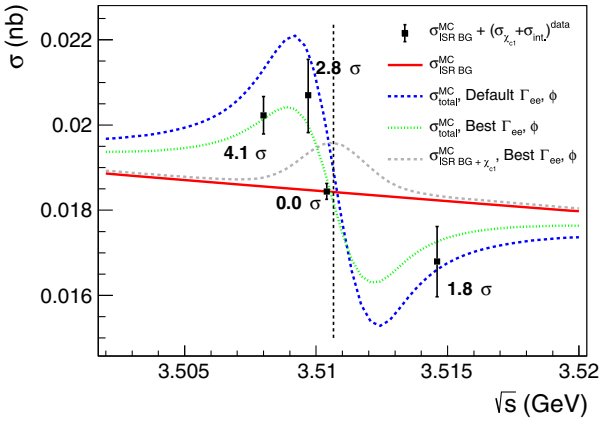

FIG. 1. The colored curves are energy-dependent cross sections of the process $e^+e^- \to \gamma J/\psi \to \gamma\mu^+\mu^-$ including (green and blue curves) and not including (red curve) the direct production of $e^+e^- \to \chi_{c1}$ (see text for more details). The gray curve denotes the signal strength in the hypothetical case of no interference. The location of the χ_{c1} mass is indicated by the vertical line. The black dots with error bars represent $\sigma^{\rm MC}_{\rm ISR\ BG} + (\sigma_{\chi_{c1}} + \sigma_{\rm int})^{\rm data}$ at the χ_{c1} scan data samples. The numbers next to the four data points indicate the statistical significances associated with the χ_{c1} production.

parity, and charge conjugation of R, respectively. In principle, C-even resonances can also be produced directly in e^+e^- annihilation through processes with two timelike virtual photons or neutral currents. Notice that the production via two real photons is forbidden due to the Landau-Yang theorem. Such processes were discussed already 40 years ago [1] and were revisited in Refs. [2–5]. Experimental searches for e^+e^- annihilation to the η, η', $f_0(980)$, $f_0(1300)$, $f_1(1285)$, $f_2(1270)$, $a_0(980)$, $a_2(1320)$, and the $X(3872)$ [also known as $\chi_{c1}(3872)$] have been carried out at the VEPP-2M [6–8], VEPP-2000 [9–11], and BEPCII [12] colliders. The most significant signal (2.5σ) was obtained for the $f_1(1285)$ [11]. All others resulted in upper limits on the electronic widths (Γ_{ee}) of the corresponding resonances. In a spacelike two-photon scattering process, $e^+e^- \to e^+e^-X(3872)$, evidence (3.2σ) for the $X(3872)$ production has also been found [13] at Belle. As for the $\chi_{c1}(1P)$, which we refer to as the χ_{c1}, there have been no previous searches.

Following the strategy for calculating the electronic width of the χ_{c1} suggested in Ref. [1], the authors of Ref. [14] predict $\Gamma_{ee} = 0.41$ eV. This work also considers the interference between the signal process, $e^+e^- \to \chi_{c1} \to \gamma J/\psi \to \gamma\mu^+\mu^-$, and the irreducible background processes $e^+e^- \to \gamma_{\rm ISR} J/\psi \to \gamma_{\rm ISR}\mu^+\mu^-$ and nonresonant $e^+e^- \to \gamma\mu^+\mu^-$, see blue and red curves in Fig. 1. Here ISR stands for initial state radiation. Depending on the value of the relative phase ϕ between the signal and background amplitudes, the interference changes the total cross section line shape dramatically.

In this Letter, we report a search for the reaction $e^+e^- \to \chi_{c1}$ at the BESIII experiment at the BEPCII collider. First, the background processes are studied and then we carry out a search for the signal process beyond the background. The data samples are collected at four center-of-mass (c.m.) energies (3.5080, 3.5097, 3.5104, and 3.5146 GeV) in the χ_{c1} mass region (referred to as the χ_{c1} scan sample) with the BESIII detector [15]. The first two scan points are located below the χ_{c1} mass, where according to Ref. [14] a constructive interference effect between the signal process and the irreducible background processes is expected. The third scan point is very slightly below the mass position, hence a minimal effect is predicted. The fourth point is above the χ_{c1} mass, which should lead to a reduction of events with respect to the scenario with no direct production of the χ_{c1}. If there was no interference, the

TABLE I. The c.m. energies, integrated luminosities, and fit results for the control samples (above the horizontal line) and for the χ_{c1} scan sample (below). The number of signal events ($N_{\rm sig}$) is obtained from a two-dimensional fit without ($N_{\rm sig}$ w/o corr.) and with ($N_{\rm sig}$ w/ corr.) the two-dimensional correction described in the text. The first uncertainty is statistical, and the second is systematic (if applied). The first value in parentheses denotes the statistical significance. The second value in parentheses for the control samples is the significance when the size of the data set is normalized to 180 pb^{-1} (thereby increasing the statistical errors); the second value for the χ_{c1} scan samples is the significance including the systematic uncertainties. The last column shows the number of signal events derived from a MC sample where the values of Γ_{ee} and ϕ are fixed to the values obtained from a common fit to all χ_{c1} scan samples (the error includes systematic effect).

$\sqrt{s}$ (MeV)	$\mathcal{L}$ (pb^{-1})	$N_{\rm sig}$ w/o corr.	$N_{\rm sig}$ w/ corr.	$N_{\rm sig}$ w/o corr. common fit
3773.0	2932.4	1027 ± 140 (7.5σ; $1.9\sigma_{180}$)	49 ± 141 (0.3σ; $0.1\sigma_{180}$)	⋯
4178.4	3192.5	522 ± 104 (5.1σ; $1.2\sigma_{180}$)	40 ± 104 (0.4σ; $0.1\sigma_{180}$)	⋯
3581.5	85.3	31 ± 29 (1.1σ; $1.6\sigma_{180}$)	-5 ± 29 (0.2σ; $0.3\sigma_{180}$)	⋯
3670.2	83.6	38 ± 26 (1.5σ; $2.2\sigma_{180}$)	4 ± 26 (0.2σ; $0.2\sigma_{180}$)	⋯
3508.0	181.8	320 ± 51 (6.5σ)	$210 \pm 52 \pm 18$ (4.1σ; $4.0\sigma_{\rm low}$)	191^{+60}_{-59}
3509.7	39.3	85 ± 24 (3.9σ)	$63 \pm 24 \pm 6$ (2.8σ; $2.7\sigma_{\rm low}$)	41^{+20}_{-19}
3510.4	183.6	100 ± 48 (1.7σ)	$0^{+16}_{-19} \pm 23$ (0.0σ; $0.0\sigma_{\rm low}$)	42^{+79}_{-77}
3514.6	40.9	-16^{+16}_{-21} (0.7σ)	$-40 \pm 22 \pm 7$ (1.8σ; $1.6\sigma_{\rm low}$)	-29^{+8}_{-10}
Combined	445.6	⋯	⋯ (5.3σ; $5.1\sigma_{\rm low}$)	⋯ (5.1σ; $4.2\sigma_{\rm low}$)

excess at the third point would be expected to be the largest (see gray line in Fig. 1). The data samples are listed in Table I. The c.m. energies are measured using a beam energy measurement system (BEMS) [16] with an uncertainty of ± 0.05 MeV and the beam-energy spread is measured to be (736 ± 27) keV. The total integrated luminosity of the four data samples is 446 pb^{-1}, which is measured using large angle Bhabha events. To verify the background description, we have also analyzed four already existing control samples, in which the signal process is absent, with a total integrated luminosity of 6294 pb^{-1}, of which two samples have a large integrated luminosity ($\sqrt{s} = 3.773$ GeV and 4.178 GeV), while the other two are comparable in size to the scan samples ($\sqrt{s} = 3.581$ GeV and 3.670 GeV), as summarized in Table I.

The χ_{c1} is reconstructed via its radiative decay $\chi_{c1} \to \gamma J/\psi$, with the subsequent decay $J/\psi \to \mu^+\mu^-$. The $J/\psi \to e^+e^-$ mode is not used due to large background from the Bhabha process ($e^+e^- \to e^+e^-$).

Monte Carlo (MC) samples are used to determine the detection efficiencies and to estimate the background contributions. Simulated samples are produced with a GEANT4-based [17] MC package, which includes the geometric description of the BESIII detector and the detector response. The PHOKHARA [18] event generator is used to describe the signal process ($e^+e^- \to \chi_{c1} \to \gamma J/\psi \to \gamma\mu^+\mu^-$), the irreducible background processes ($e^+e^- \to \gamma_{\rm ISR} J/\psi \to \gamma_{\rm ISR}\mu^+\mu^-$ and $e^+e^- \to \gamma\mu^+\mu^-$), and the interference between them. Angular distributions for the signal process are implemented into the PHOKHARA event generator using Ref. [14], while the background ISR processes are modeled using Ref. [18]. Non-$\gamma_{\rm (ISR)}\mu^+\mu^-$ background events are found to be negligible ($< 0.2\%$) by studying control samples [19] and inclusive MC simulations, which include the production of open-charm mesons, the ISR production of vector charmonium(like) states, and continuum processes.

A full reconstruction method is used to select $\gamma\mu^+\mu^-$ candidate events. The charged tracks and photons are selected with the same method as described in Ref. [19]. Muon tracks are identified by the energy they deposit in the electromagnetic calorimeter (EMC) and requiring $E_{\rm EMC} < 0.4$ GeV. A four constraint ($4C$) kinematic fit is applied with two charged tracks and one of the photons constraining the total reconstructed four momentum to that of the initial state. The photon with minimum χ^2_{4C} is chosen as the best photon candidate. As checked within a MC simulation, the probability to select a wrong photon is negligible. We require the polar angle of the best photon candidate to be $|\cos\theta_\gamma| < 0.80$ to suppress background events from ISR processes.

The verification of background description is done quantitatively by performing a two-dimensional fit to the $\mu^+\mu^-$ invariant mass ($M_{\mu^+\mu^-}$) distribution and the $|\cos\theta_\mu|$ distribution with noninterfering signal and background components, whose line shapes are extracted from the corresponding MC simulations. The signal line shape is taken from the χ_{c1} signal MC simulation at $\sqrt{s} = 3.5080$ GeV, smeared with two Gaussian functions, one to account for the resolution difference between data and MC simulations and the other for line-shape differences between different energy points. In the $\mu^+\mu^-$ invariant mass distribution, we expect the irreducible background events to feature a J/ψ peak ($e^+e^- \to \gamma_{\rm ISR} J/\psi \to \gamma_{\rm ISR}\mu^+\mu^-$) on top of a smooth distribution ($e^+e^- \to \gamma\mu^+\mu^-$). The relative sizes of these background contributions are fixed using our best estimate for the electronic width of the J/ψ ($\Gamma_{ee}^{J/\psi}$). The number of signal events ($N_{\rm sig}$) is expected to be zero in the control samples. The statistical significance of the signal contribution is determined by the difference of the best log-likelihood ($-\ln L$) value and the log-likelihood value for a fit with null-signal hypothesis. However, as summarized in the third column of Table I, nonzero values for $N_{\rm sig}$ have been found, representing a discrepancy between the data and the MC simulation of the irreducible background process. We have verified that this discrepancy is not due to differences between data and MC simulation in the experimental efficiencies, but rather can be explained by uncertainties in the input $\Gamma_{ee}^{J/\psi}$ and limitations of the PHOKHARA event generator in simulating the ISR production of the narrow J/ψ resonance for large-angle ISR photons [20]. The statistical significance of the discrepancy differs sizably for the four control samples. When normalizing the effect of the discrepancy to an integrated luminosity of 180 pb^{-1}, which corresponds to a typical luminosity of the χ_{c1} scan points, we observe significances below 2.3σ.

We carry out a two-dimensional correction to the distributions of $M_{\mu^+\mu^-}$ and $|\cos\theta_\mu|$ by reweighting MC simulated events to correct the discrepancy. The correction factors are extracted using data and MC samples at $\sqrt{s} = 3.773$ GeV or 4.178 GeV and are applied to the MC simulations at other data samples (see Supplemental Material [21]). After applying these correction factors, $N_{\rm sig}$ is consistent with zero within one standard deviation for all control samples.

In order to extract the number of signal events at the four χ_{c1} scan points, the $M_{\mu^+\mu^-}$ and $|\cos\theta_\mu|$ distributions are investigated using a similar method as above. The fit is performed at each data sample individually using a two-dimensional unbinned maximum likelihood fit method. The line shapes for the contributions from the χ_{c1} production, the irreducible background, and the interference between them are derived from the corresponding individual MC simulations (see Supplemental Material [21] for the angular distributions). The same two-dimensional correction as above is applied to the shapes of the background processes, and the square root of the same factor is used for the interference. The numbers of χ_{c1} ($N_{\chi_{c1}}$) and irreducible

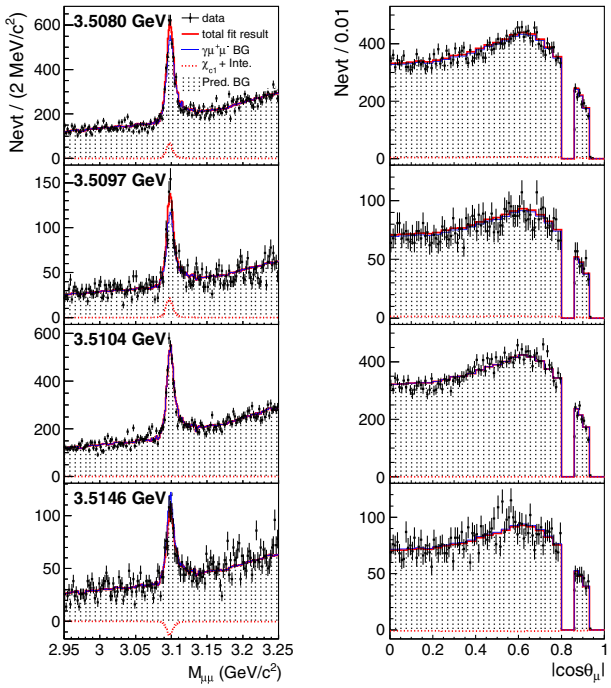

FIG. 2. One-dimensional projections of the two-dimensional fit to the $M_{\mu^+\mu^-}$ and $|\cos\theta_\mu|$ distributions from the χ_{c1} scan samples. The black dots with error bars are from data, the gray histograms are the irreducible background predicted by the corrected MC simulation. The red curve is the best fit result, the red dotted (blue dashed) curve is the signal (background) contribution. The region between $0.8 < |\cos\theta_\mu| < 0.86$ corresponds to the gap between the barrel and end cap modules of the EMC.

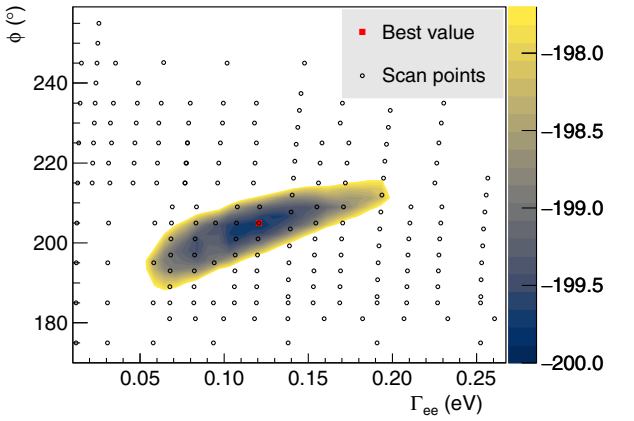

FIG. 3. The 68.3% C.L. contour of Γ_{ee} and ϕ on a distribution of log-likelihood $(-\ln L)$ values. The distribution of $-\ln L$ in a larger parameter space region is shown in Supplemental Material [21].

background events ($N_{\rm bg}$) are free parameters, while the interference ($N_{\rm int}$) is written as $f \cdot \sqrt{N_{\chi_{c1}} \cdot N_{\rm bg}}$, where the factor f is determined from signal MC sample with the Γ_{ee} and ϕ parameters set to the optimal values from a common fit to all scan points, as will be explained below.

The fit results are shown in Fig. 2 and are listed in Table I. Significant signal components are seen at $\sqrt{s} = 3.5080$ GeV and 3.5097 GeV with $N_{\rm sig} = N_{\chi_{c1}} + N_{\rm int}$ (and its statistical significance) determined to be 210 ± 52 (4.1σ) and 63 ± 24 (2.8σ), respectively. The signal component is not significant at $\sqrt{s} = 3.5104$ GeV with $N_{\rm sig} = 0^{+16}_{-19}$ (0.0σ). A negative signal component is seen at $\sqrt{s} = 3.5146$ GeV with $N_{\rm sig} = -40 \pm 22$ (1.8σ). The combined statistical significance, obtained by adding the log-likelihoods from each of the four data samples, is 5.3σ. The cross section of the signal component and its uncertainty is calculated as $\sigma_{\rm sig} \equiv (\sigma_{\chi_{c1}} + \sigma_{\rm int})^{\rm data} = N_{\rm sig}/(\mathcal{L} \cdot \epsilon)$, where the efficiency ϵ is calculated from the simulated signal MC samples. The sum of $\sigma_{\rm sig}$ and $\sigma_{\rm ISR\ BG}$ at each χ_{c1} scan point is shown in Fig. 1 (black dots), which is in good agreement with the theoretical prediction [14]. Here $\sigma_{\rm ISR\ BG}$ is fixed using the PHOKHARA generator. Statistical tests are performed to the χ_{c1} scan samples individually using likelihood ratios $t = -(\ln L_{\rm s} - \ln L_{\rm ns})$ to discriminate the hypothesis with or without signal components (distributions to be found in Supplemental Material [21]).

Using a common fit to the four χ_{c1} scan points, the values of Γ_{ee} and ϕ can be determined directly from data. Since it is not easy to obtain an analytic formula for the total cross section of $e^+e^- \to \gamma_{\rm (ISR)}\mu^+\mu^-$ as a function of Γ_{ee} and ϕ, the analysis is done via a scan method. At each c.m. energy of the χ_{c1} scan sample, the MC samples of $e^+e^- \to \gamma_{\rm (ISR)}\mu^+\mu^-$ are produced with different sets of (Γ_{ee}, ϕ) values, see open circles in Fig. 3. The total likelihood from the four samples in the χ_{c1} mass region is then calculated using the same two-dimensional distributions used previously with the number of events at each energy point constrained to the expected number of events calculated from MC. The best Γ_{ee} and ϕ parameters are determined to be $(0.12^{+0.08}_{-0.07})$ eV and $(205.0^{+10.0}_{-17.0})°$, respectively, where the uncertainty corresponding to 68.3% C.L. is statistical only. The 68.3% C.L. contour region in the (Γ_{ee}, ϕ) plane is shown in Fig. 3, in which the red dot represents the best-fitted value. The green curve in Fig. 1 shows the cross section line shape for such a set of parameters. Using this best set of (Γ_{ee}, ϕ) values, the number of signal events is estimated for each χ_{c1} scan sample and is found to be 191, 41, 42, −29 events for the four scan samples. The uncertainties on $N_{\rm sig}$ are estimated by varying the (Γ_{ee}, ϕ) values within their 68.3% C.L. contour and finding the largest variations of $N_{\rm sig}$. Combining the four samples, the statistical significance is 5.1σ and is found to be in very good agreement with the previous estimate by fitting each scan sample individually, where Γ_{ee} and ϕ are not constrained to be the same.

Systematic uncertainties for the extraction of Γ_{ee} and ϕ mainly come from the luminosity measurement, the detection efficiency, the line shapes used in the fit, the fit range, the two-dimensional correction factor, the

non-$\gamma_{(\mathrm{ISR})}\mu^+\mu^-$ background contribution, and the c.m. energy measurement.

The systematic uncertainty on the measurement of the integrated luminosity is 0.6% for each data sample. We take 0.5% as the uncertainty for muon reconstruction, which is assumed to be the same as for electron reconstruction. The uncertainty in photon reconstruction is estimated to be 0.2%, obtained using control samples of the $e^+e^- \to \gamma\mu^+\mu^-$ process. The systematic uncertainties from the integrated luminosity measurement and detection efficiency are considered simultaneously by changing the normalization factor used in the scan fit by 1.0%. The uncertainty from the requirement on $|\cos\theta_\gamma|$ is studied by tightening the requirement from 0.8 to 0.79, 0.78, 0.77, and 0.76, the largest deviation with respect to the default one is taken as the systematic uncertainty. Systematic uncertainties from other selection criteria are negligible.

The uncertainties from the binning strategy and the fit procedure are studied using toy MC samples, no bias is found. The uncertainty from the beam energy spread is considered by changing it from 736 to 1000 keV, the change is much larger than its standard deviation measured by BEMS (27 keV). The fit range of the $M_{\mu^+\mu^-}$ distribution is varied and the difference between the nominal result is considered as the systematic uncertainty. The uncertainty from the two-dimensional correction factor is estimated by replacing the nominal one extracted from the $\sqrt{s} = 3.773$ GeV data sample with that from the $\sqrt{s} = 4.178$ GeV data sample. In addition, the square root of the correction factor is applied to the interference term based on the assumption that the discrepancy observed at the control sample comes entirely from the generator level. The uncertainty from this assumption is studied by dropping the correction to the interference term. The non-$\gamma_{(\mathrm{ISR})}\mu^+\mu^-$ background contribution is neglected in the nominal fit, the uncertainty from it is considered by including it.

We change the $\sqrt{s}$ in MC simulation at each energy point by ± 0.05 MeV and take the changes as systematic uncertainty from the c.m. energy. Assuming all the systematic uncertainties are uncorrelated and adding them in quadrature, the largest parameter ranges of Γ_{ee} and ϕ corresponding to 68.3% C.L. are determined to be $(0.12^{+0.13}_{-0.08})$ eV and $(205.0^{+15.4}_{-22.4})°$, respectively. The total systematic uncertainties are of a similar size as the statistical effects. After having estimated the statistical and systematic uncertainties associated with our fit to Γ_{ee} and ϕ, we study the dependence of signal events by varying these input parameters within the contour determined at 68.3% C.L., as listed in the last column of Table I.

Systematic uncertainties for the individual fits are estimated using similar methods as listed above. However, when considering the systematic uncertainties on N_{sig}, the one on the requirement of $|\cos\theta_\gamma|$ is excluded since the signal yields change. One extra term comes from the input Γ_{ee} and ϕ values, which affect the signal line shape and is considered by varying the values within the 68.3% C.L. contour.

As summarized in Table I, we list the minimum significance found both in the case of individual fits (column "N_{sig} w/ corr.") and in the case of a common fit (column "N_{sig} w/ corr. common fit"). After including the systematic uncertainties, the minimum significance is found to be 5.1σ in the first and 4.2σ in the second case. As the significance obtained by combining individual fits is more robust to systematic effects and does not rely on the specific model of Ref. [14], we take it as our nominal result.

In summary, using data samples taken in the χ_{c1} mass region, we observe the direct production of the C-even resonance χ_{c1} in e^+e^- annihilation for the first time with a statistical significance larger than 5σ. We observe a typical interference pattern around the χ_{c1} mass, which previously was predicted in Ref. [14]. The electronic width of the χ_{c1} has been determined for the first time from a common fit to the four scan samples to be $\Gamma_{ee} = (0.12^{+0.13}_{-0.08})$ eV. This observation demonstrates that with the current generation of electron-positron colliders, the direct production of C-even resonances through two virtual photons is possible. As a next step, we intend to embark on a scan around the χ_{c2} resonance at BESIII. Using future super-tau-charm factories with increased luminosity [22], the Γ_{ee} and other properties such as the line shapes of C-even states could be determined by performing a similar scan method. This will shed light on the intrinsic nature of charmoniumlike resonances.

The BESIII Collaboration thanks the staff of BEPCII and the IHEP computing center for their strong support. We acknowledge the continuous theory support for this analysis by Henryk Czyż and Hans Kühn. This work is supported in part by National Key R&D Program of China under Contracts No. 2020YFA0406300, No. 2020YFA0406400; National Natural Science Foundation of China (NSFC) under Contracts No. 11635010, No. 11735014, No. 11835012, No. 11935015, No. 11935016, No. 11935018, No. 11961141012, No. 12022510, No. 12025502, No. 12035009, No. 12035013, No. 12192260, No. 12192261, No. 12192262, No. 12192263, No. 12192264, No. 12192265; the Chinese Academy of Sciences (CAS) Large-Scale Scientific Facility Program; Joint Large-Scale Scientific Facility Funds of the NSFC and CAS under Contracts No. U1832207, No. U2032108; CAS Key Research Program of Frontier Sciences under Contract No. QYZDJ-SSW-SLH040; 100 Talents Program of CAS; Shanghai Pujiang Program (20PJ1401700); INPAC and Shanghai Key Laboratory for Particle Physics and Cosmology; ERC under Contract No. 758462; European Union's Horizon 2020 research and innovation programme under Marie

Sklodowska-Curie grant agreement under Contract No. 894790; German Research Foundation DFG under Contracts No. 443159800, No. 455635585, Collaborative Research Center CRC 1044, GRK 2149, Research Unit FOR5327; Istituto Nazionale di Fisica Nucleare, Italy; Ministry of Development of Turkey under Contract No. DPT2006K-120470; National Science and Technology fund; STFC (United Kingdom); The Royal Society, UK under Contracts No. DH140054, No. DH160214; The Swedish Research Council; U.S. Department of Energy under Contract No. DE-FG02-05ER41374.

[a]Also at the Moscow Institute of Physics and Technology, Moscow 141700, Russia.
[b]Also at the Novosibirsk State University, Novosibirsk, 630090, Russia.
[c]Also at the NRC "Kurchatov Institute," PNPI, 188300, Gatchina, Russia.
[d]Currently at Istanbul Arel University, 34295 Istanbul, Turkey.
[e]Also at Goethe University Frankfurt, 60323 Frankfurt am Main, Germany.
[f]Also at Key Laboratory for Particle Physics, Astrophysics and Cosmology, Ministry of Education; Shanghai Key Laboratory for Particle Physics and Cosmology; Institute of Nuclear and Particle Physics, Shanghai 200240, People's Republic of China.
[g]Also at Key Laboratory of Nuclear Physics and Ion-beam Application (MOE) and Institute of Modern Physics, Fudan University, Shanghai 200443, People's Republic of China.
[h]Also at Harvard University, Department of Physics, Cambridge, Massachusetts 02138, USA.
[i]Also at State Key Laboratory of Nuclear Physics and Technology, Peking University, Beijing 100871, People's Republic of China.
[j]Also at School of Physics and Electronics, Hunan University, Changsha 410082, China.
[k]Also at Guangdong Provincial Key Laboratory of Nuclear Science, Institute of Quantum Matter, South China Normal University, Guangzhou 510006, China.
[l]Also at Frontiers Science Center for Rare Isotopes, Lanzhou University, Lanzhou 730000, People's Republic of China.
[m]Also at Lanzhou Center for Theoretical Physics, Lanzhou University, Lanzhou 730000, People's Republic of China.
[n]Also at the Department of Mathematical Sciences, IBA, Karachi, Pakistan.

[1] J. H. Kühn, J. Kaplan, and E. G. O. Safiani, Nucl. Phys. **B157**, 125 (1979); J. Kaplan and J. H. Kühn, Phys. Lett. **78B**, 252 (1978).
[2] D. Yang and S. Zhao, Eur. Phys. J. C **72**, 1996 (2012).
[3] N. N. Achasov, JETP Lett. **63**, 601 (1996).
[4] A. Denig, F. K. Guo, C. Hanhart, and A. V. Nefediev, Phys. Lett. B **736**, 221 (2014).
[5] N. Kivel and M. Vanderhaeghen, J. High Energy Phys. 02 (2016) 032.
[6] P. V. Vorobev *et al.* (ND Collaboration), Sov. J. Nucl. Phys. **48**, 273 (1988).
[7] M. N. Achasov *et al.* (SND Collaboration), Phys. Lett. B **492**, 8 (2000).
[8] M. N. Achasov *et al.* (SND Collaboration), Phys. Rev. D **98**, 052007 (2018).
[9] R. R. Akhmetshin *et al.* (CMD-3 Collaboration), Phys. Lett. B **740**, 273 (2015).
[10] M. N. Achasov *et al.* (SND Collaboration), Phys. Rev. D **91**, 092010 (2015).
[11] M. N. Achasov *et al.* (SND Collaboration), Phys. Lett. B **800**, 135074 (2020).
[12] M. Ablikim *et al.* (BESIII Collaboration), Phys. Lett. B **749**, 414 (2015).
[13] Y. Teramoto *et al.* (Belle Collaboration), Phys. Rev. Lett. **126**, 122001 (2021).
[14] H. Czyż, J. H. Kühn, and S. Tracz, Phys. Rev. D **94**, 034033 (2016).
[15] M. Ablikim *et al.* (BESIII Collaboration), Nucl. Instrum. Methods Phys. Res., Sect. A **614**, 345 (2010).
[16] J. Y. Zhang *et al.*, Chin. Phys. C **40**, 076001 (2016).
[17] S. Agostinelli *et al.* (GEANT4 Collaboration), Nucl. Instrum. Methods Phys. Res., Sect. A **506**, 250 (2003).
[18] H. Czyż, A. Grzelińska, and J. H. Kühn, Phys. Rev. D **81**, 094014 (2010).
[19] M. Ablikim *et al.* (BESIII Collaboration), Phys. Rev. D **104**, 092001 (2021).
[20] C. Carloni Calame, H. Czyz, J. Gluza, M. Gunia, G. Montagna, O. Nicrosini, F. Piccinini, T. Riemann, and M. Worek, J. High Energy Phys. 07 (2011) 126; H. Czyż (private communication).
[21] See Supplemental Material at http://link.aps.org/supplemental/10.1103/PhysRevLett.129.122001 for the $-\ln(L)$ distribution in a larger parameter space region, the two-dimensional correction factor, the fit results from the control samples, the comparison of the line shape of $|\cos\theta_\mu|$ at different c.m. energies, the scatter plots and the pull distributions from the two-dimensional fits at the χ_{c1} scan samples, and the statistical test for the discrimination of the hypothesis with or without signal components.
[22] X. R. Lyu (STCF Working Group), Proc. Sci., BEAUTY2020 (**2021**) 060.